# First Accurate Normalization of the β -delayed α Decay of N 16 and Implications for the C 12 (α,γ) O 16 Astrophysical Reaction Rate

Downloaded from: https://research.chalmers.se, 2026-10-16 18:38 UTC

Citation for the original published paper (version of record):
Kirsebom, O., Tengblad, O., Lica, R. et al (2018). First Accurate Normalization of the β -delayed α Decay of N 16 and Implications for the C 12
(α,γ) O 16 Astrophysical Reaction Rate. Physical Review Letters, 121(14).
http://dx.doi.org/10.1103/PhysRevLett.121.142701

N.B. When citing this work, cite the original published paper.

research.chalmers.se offers the possibility of retrieving research publications produced at Chalmers University of Technology. It covers all kind of research output: articles, dissertations, conference papers, reports etc. since 2004. research.chalmers.se is administrated and maintained by Chalmers Library

(article starts on next page)

# First Accurate Normalization of the $\beta$-delayed $\alpha$ Decay of $^{16}$N and Implications for the $^{12}$C$(\alpha,\gamma)^{16}$O Astrophysical Reaction Rate

O. S. Kirsebom,[1,*] O. Tengblad,[2] R. Lica,[3,4] M. Munch,[1] K. Riisager,[1] H. O. U. Fynbo,[1] M. J. G. Borge,[2,3] M. Madurga,[3] I. Marroquin,[2] A. N. Andreyev,[5,18] T. A. Berry,[6] E. R. Christensen,[1] P. Díaz Fernández,[7] D. T. Doherty,[5] P. Van Duppen,[8] L. M. Fraile,[9] M. C. Gallardo,[9] P. T. Greenlees,[10,11] L. J. Harkness-Brennan,[12] N. Hubbard,[1,5] M. Huyse,[8] J. H. Jensen,[1] H. Johansson,[7] B. Jonson,[7] D. S. Judson,[12] J. Konki,[3,10,11] I. Lazarus,[13] M. V. Lund,[1] N. Marginean,[4] R. Marginean,[4] A. Perea,[2] C. Mihai,[4] A. Negret,[4] R. D. Page,[12] V. Pucknell,[13] P. Rahkila,[10,11] O. Sorlin,[3,14] C. Sotty,[4] J. A. Swartz,[1] H. B. Sørensen,[1] H. Törnqvist,[15,16] V. Vedia,[9] N. Warr,[17] and H. De Witte[8]

[1]*Department of Physics and Astronomy, Aarhus University, DK-8000 Aarhus C, Denmark*
[2]*Instituto de Estructura de la Materia, CSIC, E-28006 Madrid, Spain*
[3]*CERN, CH-1211 Geneva 23, Switzerland*
[4]*Horia Hulubei National Institute for Physics and Nuclear Engineering (IFIN-HH), RO-077125 Bucharest-Magurele, Romania*
[5]*Department of Physics, University of York, York YO10 5DD, United Kingdom*
[6]*Department of Physics, University of Surrey, Guildford, GU2 7XH, United Kingdom*
[7]*Department of Physics, Chalmers University of Technology, S-41296 Göteborg, Sweden*
[8]*KU Leuven, Instituut voor Kern- en Stralingsfysica, 3001 Leuven, Belgium*
[9]*Grupo de Física Nuclear, Universidad Complutense de Madrid, E-28040 Madrid, Spain*
[10]*University of Jyvaskyla, Department of Physics, P.O. Box 35, FI-40014 University of Jyvaskyla, Finland*
[11]*Helsinki Institute of Physics, University of Helsinki, P.O. Box 64, FI-00014 Helsinki, Finland*
[12]*Oliver Lodge Laboratory, University of Liverpool, Liverpool L69 7ZE, United Kingdom*
[13]*STFC Daresbury, Daresbury, Warrington WA4 4AD, United Kingdom*
[14]*GANIL, CEA/DSM-CNRS/IN2P3, Bvd Henri Becquerel, 14076 Caen, France*
[15]*Institut für Kernphysik, Technische Universität Darmstadt, Darmstadt, Germany*
[16]*GSI Helmholtzzentrum für Schwerionenforschung, Darmstadt, Germany*
[17]*Institut für Kernphysik, Universität zu Köln, D-50937 Köln, Germany*
[18]*Advanced Science Research Centre (ASRC), Japan Atomic Energy Agency (JAEA), Tokai-mura, Ibaraki 319-1195, Japan*

(Received 9 April 2018; revised manuscript received 22 June 2018; published 3 October 2018)

The $^{12}$C$(\alpha,\gamma)^{16}$O reaction plays a central role in astrophysics, but its cross section at energies relevant for astrophysical applications is only poorly constrained by laboratory data. The reduced $\alpha$ width, $\gamma_{11}$, of the bound $1^-$ level in $^{16}$O is particularly important to determine the cross section. The magnitude of $\gamma_{11}$ is determined via sub-Coulomb $\alpha$-transfer reactions or the $\beta$-delayed $\alpha$ decay of $^{16}$N, but the latter approach is presently hampered by the lack of sufficiently precise data on the $\beta$-decay branching ratios. Here we report improved branching ratios for the bound $1^-$ level [$b_{\beta,11} = (5.02 \pm 0.10) \times 10^{-2}$] and for $\beta$-delayed $\alpha$ emission [$b_{\beta\alpha} = (1.59 \pm 0.06) \times 10^{-5}$]. Our value for $b_{\beta\alpha}$ is 33% larger than previously held, leading to a substantial increase in $\gamma_{11}$. Our revised value for $\gamma_{11}$ is in good agreement with the value obtained in $\alpha$-transfer studies and the weighted average of the two gives a robust and precise determination of $\gamma_{11}$, which provides significantly improved constraints on the $^{12}$C$(\alpha,\gamma)$ cross section in the energy range relevant to hydrostatic He burning.

DOI: 10.1103/PhysRevLett.121.142701

In the hot and dense interior of stars, helium is burned into carbon and oxygen by means of the triple-$\alpha$ reaction and the $^{12}$C$(\alpha,\gamma)$ reaction. The rates of the two reactions regulate the relative production of carbon and oxygen—a quantity of paramount importance in astrophysics affecting everything from grain formation in stellar winds to the late evolution of massive stars and the composition of type-Ia supernova progenitors [1]. At the temperatures characteristic of hydrostatic He burning, the triple-$\alpha$ reaction is dominated by a single, narrow resonance—the so-called Hoyle resonance—and hence it has been possible to constrain the reaction rate through measurements of the properties of the Hoyle resonance. In contrast, the $^{12}$C$(\alpha,\gamma)$

*Published by the American Physical Society under the terms of the Creative Commons Attribution 4.0 International license. Further distribution of this work must maintain attribution to the author(s) and the published article's title, journal citation, and DOI.*

reaction receives contributions from several levels in $^{16}$O, which, as it happens, all lie outside the energy window where thermal fusion of $\alpha + {}^{12}$C in the stellar environment is efficient—the so-called Gamow window. This makes the task of determining the $^{12}\mathrm{C}(\alpha,\gamma)$ rate rather complex. While the triple-$\alpha$ rate is now considered known within 10% in the energy range relevant to hydrostatic He burning [2], with efforts underway to reduce the uncertainty to 5% [3,4], the uncertainty on the $^{12}\mathrm{C}(\alpha,\gamma)$ rate was recently estimated to be at least 20%, which is insufficient for several astrophysical applications [1].

The $^{12}\mathrm{C}(\alpha,\gamma)$ cross section has been measured down to center-of-mass energies of $\approx$1.0 MeV, but the rapidly decreasing tunneling probability makes it challenging to extend the measurements to lower energies and practically impossible to reach the Gamow energy of 0.3 MeV. According to current understanding [1], the capture cross section at 0.3 MeV receives its largest single contribution from the high-energy tail of the bound $1^-$ level in $^{16}$O, situated at an excitation energy of $E_x = 7.12$ MeV only 45 keV below the $\alpha + {}^{12}$C threshold. The reduced $\alpha$ width of this level, $\gamma_{11}$, provides a measure of how strongly the level couples to the $\alpha + {}^{12}$C channel. Therefore, $\gamma_{11}$ is a critical quantity in determining the level's contribution to the capture cross section at 0.3 MeV and, more generally, in constraining the extrapolation of the $^{12}\mathrm{C}(\alpha,\gamma)$ cross section to the energy range relevant for stellar helium burning. Specifically, the dominant term in the expression for the $E1$ capture cross section [see, e.g., Eq. (6) in Ref. [5]] is proportional to $P_1\gamma_{11}^2$ where $P_1$ is the $p$-wave penetration factor of the $\alpha + {}^{12}$C channel.

The magnitude of $\gamma_{11}$ can be determined from the $\beta$-delayed $\alpha$ spectrum ($\beta\alpha$ spectrum) of $^{16}$N [6], but currently this approach is hindered by uncertainties in the normalization of the spectrum [7,8] as the inferred value for $\gamma_{11}$ is strongly correlated with the assumed $\beta$-decay branching ratios ($\gamma_{11}^2 \propto b_{\beta\alpha}/b_{\beta,11}$, see Supplemental Material [9]). Furthermore, the spectral form is not well determined experimentally due to small but significant discrepancies between existing measurements. Here, we focus our attention on the two high-precision spectra of Refs. [5,10] while disregarding a handful of other spectra, including those of Refs. [11,12], which all "retain significant experimental effects" [1].

In this Letter, we report on an experimental study of the $\beta\alpha$ decay of $^{16}$N in which the unique radioactive-isotope production capabilities of the ISOLDE facility [13] are exploited to provide the first accurate and precise determination of $b_{\beta\alpha}$. We also present a novel $R$-matrix analysis of the $\beta\alpha$ spectra of Refs. [5,10], propose a resolution to the discrepancies between the two spectra, and extract an improved value for $P_1\gamma_{11}^2$ which is in good agreement with the value inferred from sub-Coulomb $\alpha$-transfer reactions. Finally, we comment on the implications of our findings for the determination of the $^{12}\mathrm{C}(\alpha,\gamma)$ cross section at 0.3 MeV. A detailed account of the experimental work and the $R$-matrix analysis will be published separately [14].

The experiment was performed at the ISOLDE radioactive-beam facility of CERN [13]. Radioactive isotopes were produced by the impact of a 1.4 GeV proton beam on a nanostructured CaO target [15], before being ionized in a cooled plasma ion source and accelerated through an electrostatic potential difference of 30 kV. Ions with the desired mass-to-charge ($A/q$) ratio were selected in the high-resolution separator and guided to the ISOLDE decay station [16] where their decay was studied. The ions were stopped in a thin ($33 \pm 3$ $\mu$g/cm$^2$) carbon foil surrounded by five double-sided silicon strip detectors (DSSD) and four high-purity germanium (HPGe) clovers, allowing for the simultaneous detection of charged particles and $\gamma$ rays. Meanwhile, auxiliary detectors were used to check that the beam was being fully transmitted to the center of the setup and stopped in the foil. During five days of data taking, the $\beta\alpha$ decay of $^{16}$N was studied mainly on $A/q = 30$ ($^{16}\mathrm{N}^{14}\mathrm{N}^+$) but also on $A/q = 31$ ($^{16}\mathrm{N}^{14}\mathrm{N}^1\mathrm{H}^+$). Additionally, the decays of $^{17}$Ne ($\beta\gamma$, $\beta p$, $\beta\alpha$), $^{18}$N ($\beta\gamma$, $\beta\alpha$), and $^{34}$Ar ($\beta\gamma$) were studied on $A/q = 17$, 32, and 34, providing crucial data for the efficiency calibration of the HPGe array and the energy calibration of the DSSD array.

Three of the DSSDs were sufficiently thin (40 $\mu$m and 60 $\mu$m) to allow the $\alpha$ spectrum of $^{16}$N to be clearly separated from the $\beta$ background. The other two DSSDs were much thicker (300 $\mu$m and 1 mm) and served primarily to detect the $\beta$ particles. The distortions of the $\alpha$ spectrum due to $\beta$ summing was negligible due to the high granularity of the DSSDs [17]. Figure 1 shows the $\alpha$

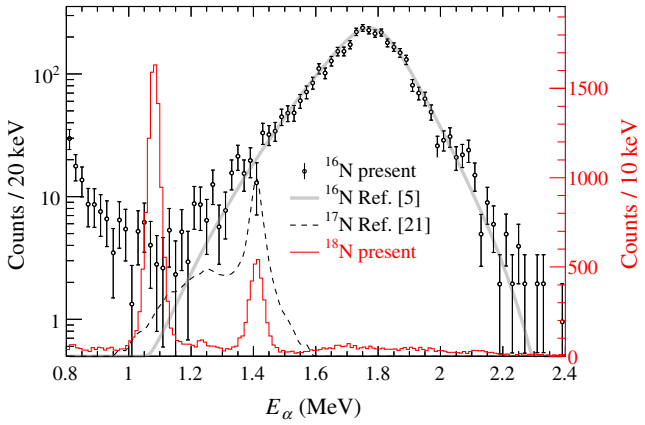


FIG. 1. $\beta$-delayed $\alpha$ spectra obtained in one of the 60 $\mu$m thick DSSDs on $A/q = 30$ (black circles) and 32 (red histogram). The two narrow $\alpha$ lines from the $\beta\alpha$ decay of $^{18}$N feature prominently in the spectrum obtained on $A/q = 32$, while the spectrum obtained on $A/q = 30$ is due almost entirely to the $\beta\alpha$ decay of $^{16}$N except for a $(2.0 \pm 0.4)\%$ contamination from the $\beta\alpha$ decay of $^{17}$N (dashed curve) which has been subtracted. The $R$-matrix fit to the $^{16}$N spectrum of Ref. [5] (downscaled and properly corrected for experimental resolution) is also shown (thick, gray curve).

spectrum obtained in one of the thin DSSDs on $A/q = 30$ during 32 hours of measurement at an average $^{16}$N implantation rate of $2 \times 10^4$ ions/s. The two narrow peaks at $E_\alpha = 1081 \pm 1$ and $1409 \pm 1$ keV in the $\beta\alpha$ spectrum of $^{18}$N [18,19] obtained on $A/q = 32$ were used to determine the detector response and energy calibration. The energy resolution was 30 keV (FWHM) for the two 60 $\mu$m DSSDs and 70 keV for the 40 $\mu$m DSSD.

The top panel of Fig. 2 shows the $\gamma$-ray spectrum measured in the HPGe clovers. The spectrum exhibits the characteristic $\gamma$ rays from the decay of $^{16}$N [20], most notably the prominent lines at 2.74, 6.13, and 7.12 MeV. Additionally, the spectrum provides evidence for only one other $\beta$-delayed particle emitter, namely, $^{17}$N, present at a level of 1.3% relative to $^{16}$N, as inferred from the observation of its 0.871 MeV and 2.18 MeV $\gamma$ rays. Based on the known $\beta\alpha$ branching ratio of $^{17}$N of $(2.5 \pm 0.4) \times 10^{-5}$ [21], we determine the level of $^{17}$N contamination in our $\alpha$ spectrum to be $(2.0 \pm 0.4)\%$. In order to convert the observed $\gamma$-ray yields to intensity ratios, it is necessary to correct for the energy dependent detection efficiency of the HPGe array. An absolutely calibrated $^{152}$Eu source was used to determine the detection efficiency at low energies, while $\beta\gamma$, $\gamma\gamma$, and $p\gamma$ coincidence data were used to extend the efficiency calibration to higher energies. A GEANT4 simulation [22], normalized only to the $^{152}$Eu data, was used to validate the efficiency calibration. As seen in Fig. 2(c), there is excellent agreement across the entire energy range. Particular attention was paid to the 6.13 MeV $\gamma$ ray since it is used for the overall normalization. Using the $\gamma\gamma$ coincidences due to the $8.87 \rightarrow 6.13 \rightarrow$ g.s. cascade [Fig. 2(b)] and $\beta\gamma$ coincidences, the detection efficiency at 6.13 MeV was determined with a precision of 1.4%. After correcting the observed $\gamma\gamma$ coincidence yield for the known angular correlation [23], the two approaches ($\gamma\gamma$ and $\beta\gamma$) gave fully consistent results.

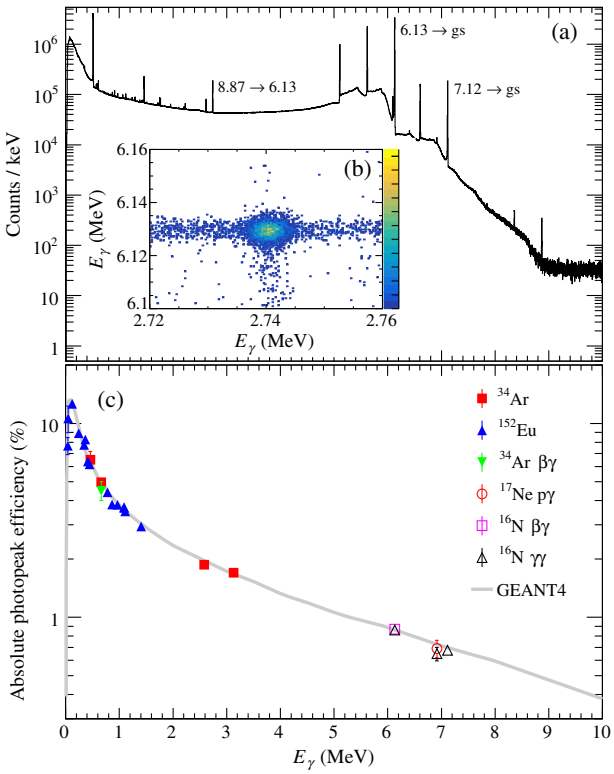


FIG. 2. (a) $\gamma$-ray spectrum from the $\beta$ decay of $^{16}$N with main transitions indicated. (b) $\gamma\gamma$ coincidence spectrum zoomed in on the $8.87 \rightarrow 6.13 \rightarrow$ g.s. cascade. (c) Experimentally determined and simulated $\gamma$-ray detection efficiency.

Based on the relative $\gamma$-ray yields, we determine the $\beta$-decay branching ratio to the 7.12 MeV level in $^{16}$O to be $b_{\beta,11} = (5.02 \pm 0.10) \times 10^{-2}$ in agreement with Refs. [10,20,24–26], but with a reduced uncertainty due to the precise efficiency calibration and high energy resolution of the present study. Based on the number of detected $\alpha$ particles, the measured 6.13 MeV $\gamma$-ray yield, and the known relative intensity of the 6.13 MeV $\gamma$-ray line ($0.670 \pm 0.006$ [20,27,28]), we determine the branching ratio for $\alpha$ emission to be $b_{\beta\alpha} = (1.59 \pm 0.06) \times 10^{-5}$ with the following error budget: $\alpha$-particle detection efficiency, 3.0%; $\gamma$-ray detection efficiency, 1.4%; $\alpha$-particle counting uncertainty, 1.3%; tabulated intensity of the 6.13-MeV $\gamma$ ray, 0.9%; and subtraction of the $^{17}$N contamination, 0.4%. When added in quadrature these uncertainties combine to give the quoted total uncertainty of 3.8% on $b_{\beta\alpha}$. Our value for $b_{\beta\alpha}$ is significantly larger than the literature value of $(1.20 \pm 0.05) \times 10^{-5}$ [20,29], but consistent with the less precise values of $(1.3 \pm 0.3) \times 10^{-5}$ obtained by Ref. [30] and $[1.49 \pm 0.05(\text{stat})^{+0.0}_{-0.10}(\text{sys})] \times 10^{-5}$ obtained by us in a previous study using a different experimental technique [31].

In order to parametrize the shape of the $\alpha$ spectrum, we adopt an $R$-matrix model similar to that of Refs. [5,10], consisting of two physical $p$-wave levels at $E_x = 7.12$ and 9.59 MeV, two physical $f$-wave levels at $E_x = 6.13$ and 11.60 MeV, and a $p$-wave background pole at higher energy. The $R$-matrix model of Refs. [5,10] additionally includes an $f$-wave background pole with zero feeding, but we find that the inclusion of such a pole only gives a marginal improvement of $\chi^2$ and a slightly worse $\chi^2/N$ and hence we do not include it. On the other hand, we allow the feeding of the 11.60 MeV level, which was also set to zero in Refs. [5,10], to vary freely. Our analysis differs from those of Refs. [5,10] in a few significant respects: first and most importantly, the analyses of Refs. [5,10] were aimed at determining the capture cross section at 0.3 MeV and therefore involved the simultaneous fitting of $\beta\alpha$-decay data, $\alpha$-scattering data, and $\alpha$-capture data. Our analysis, on the other hand, is aimed at determining the constraints imposed on $\gamma_{11}$ by the $\beta\alpha$-decay data alone and at resolving the discrepancies between Refs. [5,10], and hence we restrict our attention to the $\beta\alpha$-decay data. We also

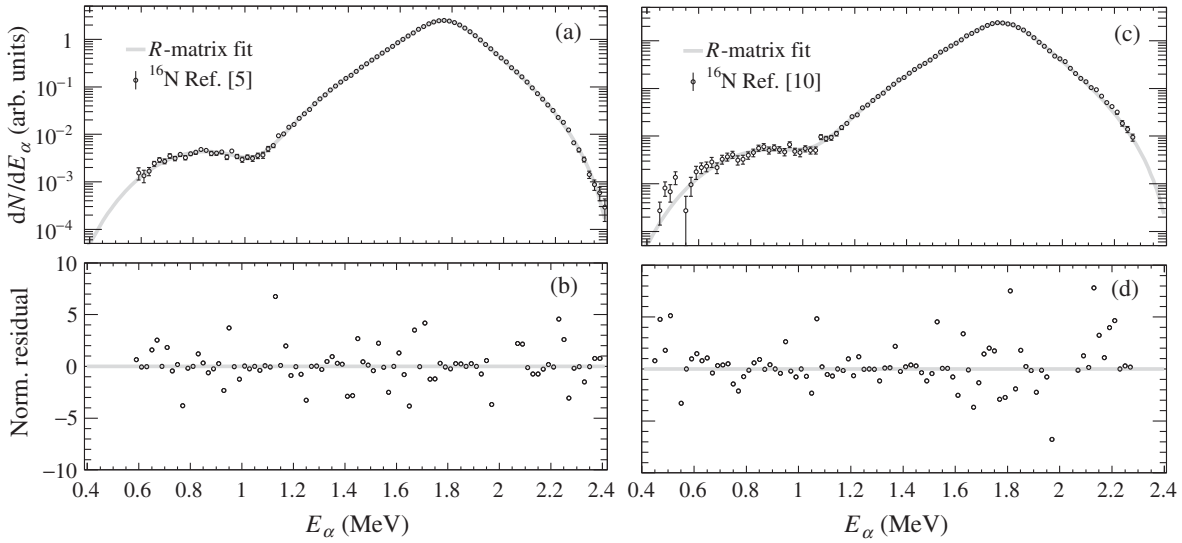


FIG. 3. (a), (c) $R$ matrix fits to the $\beta\alpha$ spectra of Refs. [5,10]. (b), (d) Normalized residuals.

adopt our improved values for $b_{\beta,11}$ and $b_{\beta\alpha}$, and we fix the asymptotic normalization coefficient (ANC) of the 6.13 MeV level to the rather precise value of $C = 139 \pm 9$ fm$^{-1/2}$ inferred from sub-Coulomb transfer reactions [32]. All $R$-matrix calculations have been performed with the code ORM [33]. Further details are provided in the Supplemental Material [9].

Following Refs. [5,10] we ignore the four data points in the vicinity of the narrow $2^+$ level at $E_x = 9.68$ MeV. Allowing the channel radius to vary, we obtain a very good fit to the spectrum of Ref. [5] ($\chi^2/N = 94.3/79 = 1.19$, $P_{\chi^2>94.3} = 0.116$, Fig. 3 left panel) yielding

$$P_1\gamma_{11}^2 = 5.17 \pm 0.75(\text{stat}) \pm 0.54(\text{sys})\ \mu\text{eV}, \qquad (1)$$

(with $P_1$ evaluated at 0.3 MeV) and a preferred channel radius of 6.35 fm. The largest contribution to the systematic uncertainty comes from the energy calibration (3.8%) with smaller contributions from $b_{\beta\alpha}$ (2.7%) and $b_{\beta,11}$ (2.0%) and even smaller contributions from the subtraction of $^{17}$N and $^{18}$N impurities (1.0%), the ANC of the 6.13 MeV level (0.4%), and the energy resolution (0.3%). Using the old branching ratio of $b_{\beta\alpha} = 1.20 \times 10^{-5}$ [20,29], we obtain $P_1\gamma_{11}^2 = 3.92 \pm 0.57(\text{stat})\ \mu$eV with no change in fit quality. Thus, our revised value for $b_{\beta\alpha}$ leads to a 32% increase in $P_1\gamma_{11}^2$. The precise effect on the $E1$ capture cross section is difficult to determine since it requires a simultaneous fit to the $\beta\alpha$ spectrum, $\alpha$-capture data, and $\alpha$-scattering data, which is beyond the scope of the present study. An accurate estimate can, however, be obtained by adopting the best-fit parameters of Ref. [5] and only modify the value of $\gamma_{11}$. Doing so, one finds a 24% increase in the $E1$ capture cross section at 0.3 MeV, implying an upward shift of the best estimate of the astrophysical $S$ factor from $S_{E1}(0.3) = 79$ keV b [5] to $S_{E1}(0.3) = 98$ keV b.

We are unable to obtain a satisfactory fit to the spectrum of Ref. [10] ($\chi^2/N = 114.9/79 = 1.45$, $P_{\chi^2>114.9} = 0.005$, Fig. 3 right panel). Also, the channel radius preferred by the fit is significantly smaller (5.35 fm). Yet, we obtain $P_1\gamma_{11}^2 = 6.82 \pm 0.65(\text{stat})\ \mu$eV in fair agreement with Eq. (1). Given the discrepancies between the two spectra [34], it is a little surprising that we obtain almost agreeing values for $P_1\gamma_{11}^2$. As seen in Fig. 4, the dip around $E_\alpha = 1.0$ MeV is less pronounced in the spectrum of Ref. [10], and the main peak is slightly wider and shifted by $-6$ keV relative to the spectrum of Ref. [5]. However, a detailed analysis reveals the agreement to be little more than a lucky coincidence: the less pronounced dip favors a larger $\gamma_{11}$ value, but the downward energy shift has the opposite effect on $\gamma_{11}$, so the two differences almost cancel out.

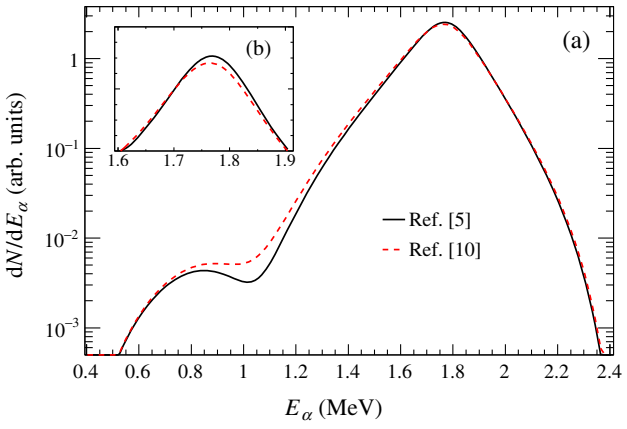


FIG. 4. (a) Comparison of the $R$-matrix distributions determined from the $\beta\alpha$ spectra of Refs. [5,10]. (b) Zoom in on the maximum of the distribution.

The spectrum obtained in the present work contains significantly fewer counts ($1.07 \times 10^4$) than the spectra of Refs. [5,10] ($1.03 \times 10^6$ and $2.75 \times 10^5$), and hence does not impose any useful constraints on $P_1\gamma_{11}^2$. Our spectrum does, however, impose useful constraints on the position of the maximum of the $R$-matrix distribution. Taking into account the uncertainty on the energy calibration, the maximum is found to be consistent with Ref. [5], but shifted by $6 \pm 3$ keV relative to Ref. [10]. Apart from this small shift, our spectrum is consistent with both previous spectra as the level of statistics is insufficient to reveal the small discrepancies in the region around $E_\alpha = 1.0$ MeV. Thus, our analysis shows that the spectrum of Ref. [5] is both supported by the better fit quality and in better agreement with the energy calibration of the present spectrum.

Sub-Coulomb $\alpha$-transfer reactions provide an alternative route to determining $P_1\gamma_{11}^2$ by constraining the ANC of the 7.12 MeV level, which is related to $\gamma_{11}$ via Eq. (44) in Ref. [1]. Adopting the most recent and most precise ANC value of $(4.39 \pm 0.59) \times 10^{28}$ fm$^{-1}$ [32] and assuming the channel radius to be $6.32 \pm 0.27$ fm (the 68.3% confidence interval determined from the $\beta$-decay data, see the figure in the Supplemental Material [9]), we obtain $P_1\gamma_{11}^2 = 4.44 \pm 0.70$ $\mu$eV in good agreement with Eq. (1). The weighted average of the two is $4.71 \pm 0.56$ $\mu$eV, when statistical and systematic uncertainties are combined in quadrature, yielding a relative uncertainty of 12%. We note that the less precise ANCs obtained in three previous $\alpha$-transfer studies are in good agreement with that of Ref. [32].

In conclusion, we have obtained the first accurate normalization of the $\beta$-delayed $\alpha$ spectrum of $^{16}$N and resolved a significant discrepancy between two previous high-precision measurements of the spectral shape. The branching ratio for $\beta$-delayed $\alpha$ emission is found to be 33% larger than previously held and the value of $P_1\gamma_{11}^2$ inferred from the $\beta\alpha$ spectrum is increased by the same factor. Our value for $P_1\gamma_{11}^2$ is in good agreement with the value inferred from sub-Coulomb $\alpha$-transfer studies and has comparable precision. The weighted average of the two has an uncertainty of 12%. Since the dominant term in the expression for the $E1$ capture cross section is proportional to $P_1\gamma_{11}^2$, our result implies that indirect measurements alone now constrain the $E1$ capture cross section to within close to 12%, a remarkable result considering the large variability in the $S_{E1}(0.3)$ values reported over the last 60 years (Table IV of Ref. [1]). By further including direct measurements of the capture cross section as well as $\alpha$-scattering data it may be possible to reduce the uncertainty even further. Considering the progress made in recent years in constraining the other components of the $^{12}C(\alpha,\gamma)$ cross section, it may finally be possible to bring the uncertainty on the total cross section at 0.3 MeV below 10%.

We are grateful to the ISOLDE technical staff for providing excellent running conditions during the experiment, and thank the anonymous reviewers for their valuable comments and suggestions to improve the quality of the Letter. This work has been supported by the European Research Council under the ERC starting Grant Long Beamtime Experiments in Nuclear Astrophysics, No. 307447, the Horizon 2020 Research and Innovation Programme under Grant Agreement No. 654002, the Spanish Ministry of Economy and Competitiveness through Projects No. FPA2015-64969-P, FPA2015-65035-P, and FPA2017-87568-P, the Romanian Institutul de Fizica Atomica Grant CERN/ISOLDE, the United Kingdom Science and Technology Facilities Council, the Fonds voor Wetenschappelijk Onderzoek-Vlaanderen (Belgium) and GOA/2010/010 (Bijzonder OnderzoeksFonds KU Leuven), the German Federal Ministry of Education and Research under Contract No. 05P15PKCIA (ISOLDE) and Verbundprojekt 05P2015. B. J. acknowledges support from The Royal Society of Arts and Sciences in Gothenburg and OSK from the Villum Foundation through Project No. 10117.

*Corresponding author.
oliskir@phys.au.dk

[1] R. J. deBoer *et al.*, Rev. Mod. Phys. **89**, 035007 (2017).
[2] H. O. U. Fynbo and C. A. Diget, Hyperfine Interact. **223**, 103 (2014).
[3] C. Tur *et al.*, Nucl. Instrum. Methods Phys. Res., Sect. A **594**, 66 (2008).
[4] T. Kibédi, A. E. Stuchbery, G. D. Dracoulis, and K. A. Robertson, EPJ Web Conf. **35**, 06001 (2012).
[5] R. E. Azuma *et al.*, Phys. Rev. C **50**, 1194 (1994).
[6] F. C. Barker, Aust. J. Phys. **24**, 771 (1971).
[7] J. Humblet, B. W. Filippone, and S. E. Koonin, Phys. Rev. C **44**, 2530 (1991).
[8] L. Buchmann, G. Ruprecht, and C. Ruiz, Phys. Rev. C **80**, 045803 (2009).
[9] See Supplemental Material at http://link.aps.org/supplemental/10.1103/PhysRevLett.121.142701 for details on the experimental resolution of the $\alpha$ spectrum, the $R$ matrix parametrization, and the confidence limits analysis.
[10] X. D. Tang *et al.*, Phys. Rev. C **81**, 045809 (2010).
[11] H. Hättig, K. Hünchen, and H. Wäffler, Phys. Rev. Lett. **25**, 941 (1970).
[12] R. H. France III, E. L. Wilds, J. E. McDonald, and M. Gai *et al.*, Phys. Rev. C **75**, 065802 (2007).
[13] R. Catherall *et al.*, J. Phys. G **44**, 094002 (2017).
[14] O. S. Kirsebom *et al.* (to be published).
[15] J. Ramos *et al.*, Nucl. Instrum. Methods Phys. Res., Sect. B **320**, 83 (2014).
[16] H. Fynbo, O. S. Kirsebom, and O. Tengblad, J. Phys. G **44**, 044005 (2017).
[17] O. S. Kirsebom *et al.*, Phys. Rev. C **83**, 065802 (2011).
[18] K. I. Hahn, C. R. Brune, and P. R. Wrean, Phys. Rev. C **48**, 914 (1993).
[19] D. Tilley, H. Weller, and C. Cheves, Nucl. Phys. **A564**, 1 (1993).
[20] D. Tilley, H. Weller, C. Cheves, and R. Chasteler, Nucl. Phys. **A595**, 1 (1995).

[21] M. Dombsky *et al.*, Phys. Rev. C **49**, 1867 (1994).
[22] C. Sotty and R. Lica (to be published).
[23] W. J. Vermeer and A. R. Poletti, J. Phys. G **8**, 743 (1982).
[24] C. H. Millar, G. A. Bartholomew, and B. B. Kinsey, Phys. Rev. **81**, 150 (1951).
[25] B. J. Toppel, Phys. Rev. **103**, 141 (1956).
[26] D. E. Alburger, A. Gallmann, and D. H. Wilkinson, Phys. Rev. **116** (1959) 939.
[27] E. K. Warburton, D. E. Alburger, and D. J. Millener, Phys. Rev. C **29**, 2281 (1984).
[28] A. R. Heath and G. T. Garvey, Phys. Rev. C **31**, 2190 (1985).
[29] W. Kaufmann and H. Wäffler, Nucl. Phys. **24**, 62 (1961).
[30] Z. Zhao, R. H. France, K. S. Lai, M. Gai, E. L. Wilds, R. A. Kryger, J. A. Winger, and K. B. Beard, Phys. Rev. C **48**, 429 (1993).
[31] J. Refsgaard *et al.*, Phys. Lett. B **752**, 296 (2016).
[32] M. L. Avila, G. V. Rogachev, E. Koshchiy, L. T. Baby, J. Belarge, K. W. Kemper, A. N. Kuchera, A. M. Mukhamedzhanov, D. Santiago-Gonzalez, and E. Uberseder, Phys. Rev. Lett. **114**, 071101 (2015).
[33] M. Munch, O. S. Kirsebom, and J. Refsgaard, 2018, DOI: 10.5281/zenodo.1174079.
[34] Possible reasons for the discrepancies between the $\beta\alpha$ spectra of Refs. [5,10] are discussed in Ref. [8].